NANOSYSTEMS:
PHYSICS, CHEMISTRY, MATHEMATICS

Chuvilo Y., et al. *Nanosystems: Phys. Chem. Math.*, 2025, **16** (6), 812–817.
http://nanojournal.ifmo.ru
DOI 10.17586/2220-8054-2025-16-6-812-817

Original article

Features of Ce(IV) phosphate coatings formation on the silica surface during their synthesis by successive ionic layer deposition method

Yuliana Chuvilo[1,a], Leonid Kuklo[1,b], Valeri Tolstoy[1,c]

[1]Institute of Chemistry, Saint Petersburg State University, University St. 26, St. Peterhof, Saint Petersburg, 198504, Russia

[a]st087011@student.spbu.ru, [b]lenkuklo@mail.ru, [c]v.tolstoy@spbu.ru

Corresponding author: Tolstoy V., v.tolstoy@spbu.ru

PACS 78.30.Lx, 78.40.Kc

ABSTRACT The article presents the conditions for obtaining Ce(IV) phosphate coatings on the surface of silicon and quartz by the successive ionic layer deposition (SILD) method. It has been shown that when using solutions of $(NH_4)_4Ce(SO_4)_4$ and NaH_2PO_4 as reagents, coatings of the composition $Ce(OH)PO_4 \cdot nH_2O$ are formed on the surface of the substrates, and when using solutions of $(NH_4)_4Ce(SO_4)_4$ and Na_3PO_4, coatings of the composition $Na_{0.2}Ce(OH)_{2.4}(PO_4)_{0.6} \cdot nH_2O$ are formed. These compounds have an amorphous structure. SEM analysis of $Na_{0.2}Ce(OH)_{2.4}(PO_4)_{0.6} \cdot nH_2O$ on the silicon surface showed that for the samples obtained as a result of 15 SILD cycles, the planar isotropic coatings are rolled into microtubules with a microscroll morphology of 3–5 μm in diameter and 30–100 μm in length. The composition of the noted Ce(IV) phosphates can be relatively easily doped during the synthesis process, for example, with Fe(II) cations and tungstate anions. It was found that $Ce(OH)PO_4 \cdot nH_2O$ coatings are characterized by intense absorption band in the UV region of the spectrum, and can be used as components in various types of absorbers. Moreover, the degree of absorption can be controlled by varying the number of synthesis conditions, for example, the number of SILD cycles.

KEYWORDS Ce(IV) phosphates, coatings, SILD, UV shielding, microscrolls.

ACKNOWLEDGEMENTS This work was supported by the RSF grant (project # 23-19-00566). We are grateful to the "Nanotechnology Centre" of Saint-Petersburg State University for technical assistance in the study of the synthesized samples.

FOR CITATION Chuvilo Y., Kuklo L., Tolstoy V. Features of Ce(IV) phosphate coatings formation on the silica surface during their synthesis by successive ionic layer deposition method. *Nanosystems: Phys. Chem. Math.*, 2025, **16** (6), 812–817.

1. Introduction

Rare earth element phosphates are known to exhibit a variety of practically important properties, and their study has received considerable attention [1–5]. Among these, Ce(IV) phosphates occupy a special place, exhibiting properties similar in many ways to those of other metal phosphates in the 4+ oxidation state, such as Ti(IV) and Zr(IV) phosphates. The conditions for the synthesis of Ce(IV) phosphates and the features of their chemical structure, as well as the results of studying their properties, are described in a number of reviews, for example in articles [6–8]. In particular, $Ce(PO_4)(HPO_4)_{0.5}(H_2O)_{0.5}$ is an active adsorbent for many environmentally unsafe metal cations, including radioactive ones [9]. Phosphates and Ce(IV) oxide are also actively studied as so-called nanozymes for biologically active processes in living organisms [10–12].

Significant results were obtained in studying the characteristics of UV radiation absorption by Ce(IV) phosphates [13, 14]. It is known that the main inorganic components of various types of creams for skin protection from UV radiation are titanium and zinc oxides, because they are characterized, on the one hand, by high absorption coefficients [15, 16] in this spectral region, and, on the other hand, they are uncolored in the visible region of the spectrum.

A similar function can be performed by cerium (IV) oxide. When irradiated with UV light, it does not generate active forms of oxygen that damage the skin, unlike titanium and zinc oxides.

In [17], it was shown that Ce(IV) phosphate exhibits properties similar to CeO_2, and in this regard, it is of interest to create new approaches to their synthesis. Another important aspect in assessing the possibility of replacing titanium and zinc oxides in creams with Ce(IV) oxide or phosphate is the need to consider the comparatively high price of cerium compounds. Therefore, such synthesis methods that allow deposition Ce(IV) phosphate coatings to various more accessible substrates are acquiring great importance. It is assumed that using these methods it is possible to obtain, for example, core-shell structures in which the content of the more expensive component is lower.

Such methods include the SILD method [18], which allows the synthesis of a wide range of inorganic compounds on the surface of complex-shaped substrates and relatively precise control of their thickness. The essence of this method is to treat the substrate according to a special program using solutions of 2 or more reagents, with intermediate rinsing of the sample with excess reagent and reaction products, using a solvent, specifically, water for aqueous solutions. The conditions of such treatments are selected in such a way that during treatment with each reagent, alternate adsorption of cations and anions occurs on the surface. It is important that these ions interact with each other and form a poorly soluble compound.

The aim of this work was to study the features of the synthesis of Ce(IV) phosphate coatings on the surface of model silica substrates represented by fused quartz samples and an ultra-thin layer of silicon oxide on the surface of single-crystal silicon. An important part of the work consisted of the results of studying the degree of absorption of UV radiation by such coatings.

2. Experimental

2.1. Materials

Aqueous solutions of $(NH_4)_4Ce(SO_4)_4 \cdot 2H_2O$, $(NH_4)_2Fe(SO_4)_2 \cdot 6H_2O$, Na_2WO_4, NaH_2PO_4 and Na_3PO_4 (JSC Lenreactive) were used as reagents for synthesis. The weighed portions of the reagents were dissolved in deionized water, stirring for at least 30 minutes. The synthesis substrates used were single crystalline silicon with $<111>$ orientation, as well as fused quartz plates measuring 10×25 mm and 0.35 and 1.0 mm thick, respectively. Before synthesis, all substrates were rinsed twice for 10 minutes using an ultrasonic bath with isopropyl alcohol. They were then washed with deionized water and dried at 60°C for 10 minutes in the air.

2.2. SILD synthesis conditions

The coatings were synthesized using a custom-made automated setup. In the first stage of the SILD synthesis, the substrate plates were immersed in a solution of $(NH_4)_4Ce(SO_4)_4$ with a concentration of 0.01 M. They were then removed from this solution and immersed in distilled water to remove excess reagent and reaction products from the surface. In the second stage, the plates were immersed in a solution of NaH_2PO_4 or Na_3PO_4 with a concentration of 0.01 M and again washed in distilled water. This sequence corresponds to one SILD cycle, which was repeated 5–25 times. A number of syntheses were performed using a solution of a mixture of $(NH_4)_4Ce(SO_4)_4$ and $(NH_4)_2Fe(SO_4)_2$, as well as Na_3PO_4 and Na_2WO_4 as one of the reagents. The treatment time in the reagent solutions and water was 30s. The synthesis was carried out at room temperature and atmospheric pressure. After deposition, the samples were dried in the air at the temperature 60°C.

2.3. Physical characterization

Scanning electron microscopy (SEM), transmission electron microscopy (TEM), scanning transmission electron microscopy (STEM), selected area electron diffraction (SAED), energy-dispersive x-ray (EDX) microanalysis, Fourier-transform infrared spectroscopy (FT-IR) and diffuse reflection (DR) spectroscopy in the UV-Vis region were used to study the synthesized samples.

Electron micrographs were obtained using a Zeiss EVO-40EP scanning microscope and a Zeiss Libra 200 transmission microscope. The synthesized compounds composition was determined by EDX microanalysis using an Oxford INCA-350 spectrometer included in the Zeiss EVO-40EP scanning electron microscope kit. The FT-IR spectra of the coatings on the silicon surface were recorded on FSM-2201 spectrophotometer according to a differential scheme relative to a pure silicon substrate. The number of scans was 60. DR spectra were obtained using a Perkin-Elmer Lambda 9 spectrophotometer equipped with an integrating sphere. When obtaining DR spectra, fused quartz plates were used as substrates. The surface of these plates was pre-polished using SiC powder with a particle size of about 20 μm as an abrasive.

3. Results and discussion

As follows from the electron micrographs shown in Fig. 1(a,b), as a result of synthesis using solutions of $(NH_4)_4Ce(SO_4)_4$ and NaH_2PO_4, continuous thin films are formed on the silicon surface, which have separate microcracks that are not through the thickness and have sizes of fractions of a micrometer. The latter may possibly form during drying of the samples in air. If a solution of Na_3PO_4 is used instead of a solution of NaH_2PO_4, then for the samples obtained as a result of 5, 10, 20 and 25 SILD cycles, such a planar morphology of the films is preserved. It is only noteworthy that the surface of such thin films has a more clearly expressed globular morphology and the sizes of such planar globules are approximately 30–100 nm. However, for the sample obtained as a result of 15 SILD cycles, the morphology of the coating changes significantly and the formation of microtubes with the morphology of microscrolls with a diameter of about 3–5 μm and a length of 30–100 μm is observed on the surface (Fig. 1(c-f)). The wall thickness of such microtubes is 50–80 nm and this indicates that during the synthesis as a result of 1 SILD cycle, a nanolayer with a thickness of $\sim$4 nm is formed on the surface. This value significantly exceeds the total dimensions of the elementary polyhedron in Ce(IV)

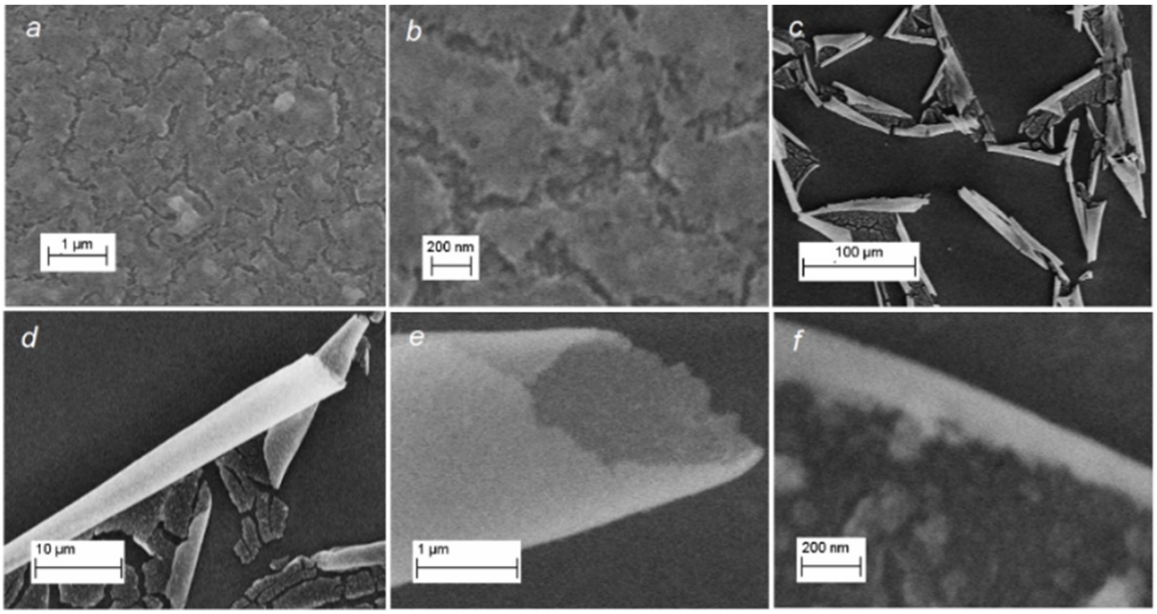

FIG. 1. SEM images of the surface of the coatings deposited on silicon wafers. a, b – the reagents in the synthesis were $(NH_4)_4Ce(SO_4)_4$ and NaH_2PO_4 solutions; c-f – $(NH_4)_4Ce(SO_4)_4$ and Na_3PO_4 solutions. The number of SILD cycles (N) was 15

oxyhydroxide and phosphate anion. This circumstance, in our opinion, indicates super-equivalent adsorption of Ce(IV) cations or phosphate anions on the surface at each stage of substrate treatment in reagent solutions.

In Fig. 1(c-f), it can be seen that the outer side of the microtube wall has a smoother surface than the inner one and the planar thin film itself is rolled up with the outer side relative to the substrate into the microtube.

Important information about the structural and chemical features of the synthesized coatings can be obtained from the analysis of electron STEM and TEM micrographs (Fig. 2(a,b)). According to these micrographs, the walls of such microtubes consist of individual nanoparticles 20–40 nm in size and these nanoparticles are amorphous (Fig. 2(c)). Similar micrographs and SAED pattern were also obtained for the coating synthesized using the NaH_2PO_4 solution and therefore we do not show them in this figure.

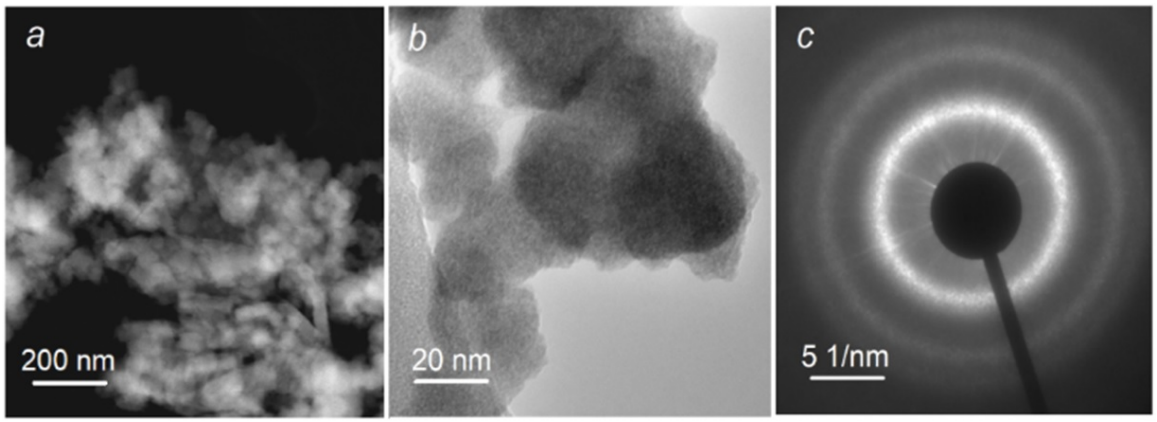

FIG. 2. STEM (a) and TEM (b) images of fragments of the coating synthesized on the silicon surface as a result of its treatment for 15 cycles with solutions of $(NH_4)_4Ce(SO_4)_4$ and Na_3PO_4 using the SILD method. (c) – typical SAED pattern of this sample

The study of the coating composition by the EDX method showed that in the case of using solutions of $(NH_4)_4Ce(SO_4)_4$ and NaH_2PO_4 for synthesis, a thin film is formed on the surface, which consists only of Ce, P and O atoms, and the ratio of Ce:P concentrations is close to 1 (Fig. 3(a)). Unfortunately, it is impossible to determine the relative content of O atoms in such thin film, because oxygen is also present in it as part of water molecules. If a solution of Na_3PO_4 is used as one of the reagents during synthesis, then in the composition of the coating, along with the noted elements, Na atoms can also be found, and the ratio of the concentrations of Na, Ce and P atoms is 0.2:1.0:0.6.

The composition of the coatings was also studied by FT-IR spectroscopy (Fig. 4(a)), the results of which indicate the presence of water molecules (absorption bands of water molecules are not shown in the figure) and phosphate anions in

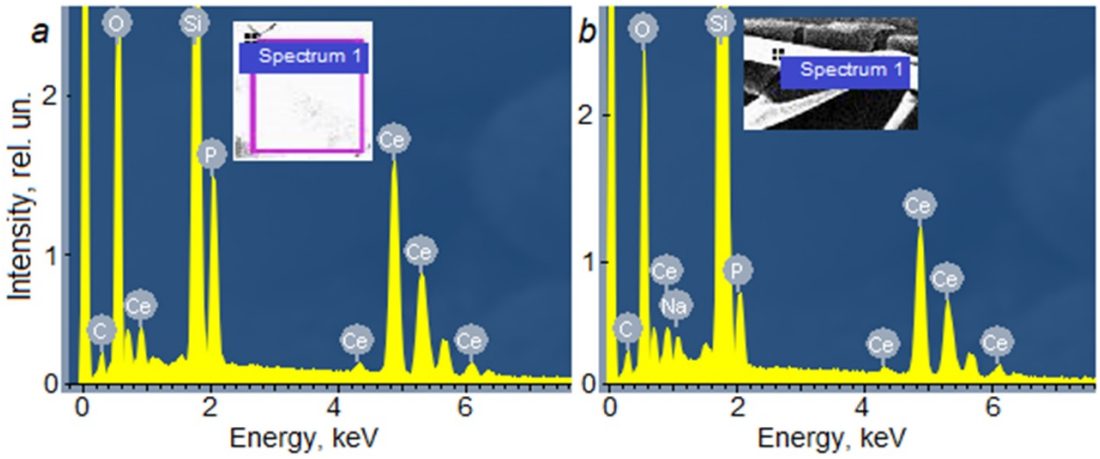

FIG. 3. EDX spectra of coatings deposited on silicon wafers. a – solutions of $(NH_4)_4Ce(SO_4)_4$ and NaH_2PO_4 served as reagents in the synthesis; b – solutions of $(NH_4)_4Ce(SO_4)_4$ and Na_3PO_4. N= 15

the layer. The presence of the latter is indicated by absorption bands in the region of 1200–900 cm^{-1} of valence and in the region of 700–500 cm^{-1} of deformation vibrations of P–O bonds [16].

Thus, the composition of the obtained coatings can be characterized by analogy with papers [19–22] as $Ce(OH)PO_4 \cdot nH_2O$ and $Na_{0.2}Ce(OH)_{2.4}(PO_4)_{0.6} \cdot nH_2O$.

A rather logical result is a slightly lower content of phosphate anions in the sample obtained using the Na_3PO_4 solution in relation to the content of the series. This solution has a significantly higher equilibrium pH value and therefore, when the substrate is immersed in it, two competing reactions are observed, namely, a more complete hydrolysis of the adsorbed Ce(IV) cations with the formation of Ce(IV) hydroxide and the adsorption of phosphate anions. In such a solution, there are also significantly more Na^+ cations and therefore, along with the adsorption of phosphate anions, adsorption of these cations is also observed. The presence of such polyionic adsorption leads to the so-called "super-equivalent" adsorption and therefore, with each SILD cycle, cations and anions are adsorbed on the surface in an amount greater than one monolayer.

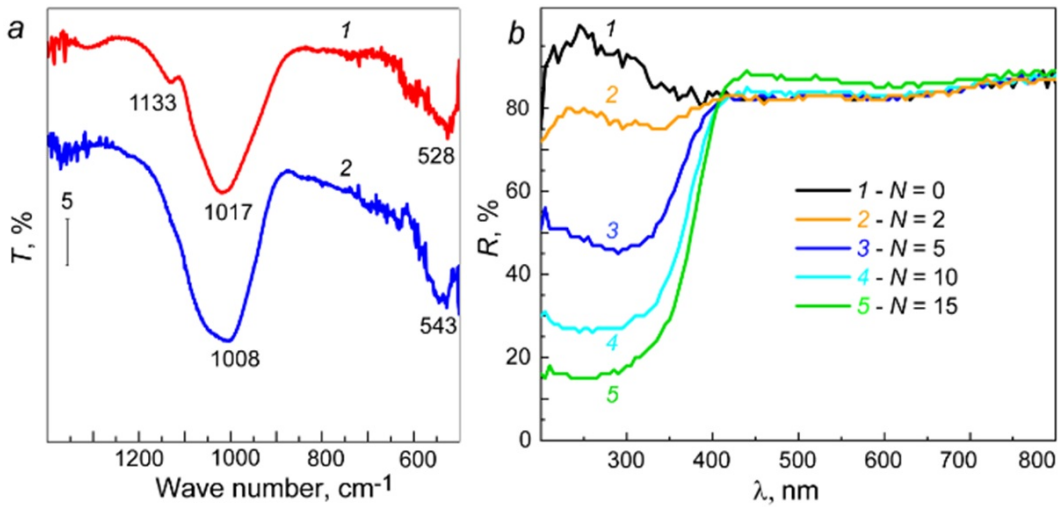

FIG. 4. a – FT-IR spectra of Ce(IV) phosphate coatings on silicon surface obtained using solutions of $(NH_4)_4Ce(SO_4)_4$ and NaH_2PO_4 (1) and $(NH_4)_4Ce(SO_4)_2$ and Na_3PO_4 (2). N= 20; b – DR UV-Vis spectra of Ce(IV) phosphate coatings on quartz surface obtained using $(NH_4)_4Ce(SO_4)_4$ and NaH_2PO_4 solutions

When discussing the obtained results, it is also necessary to interpret the effect of formation of microtubes with walls of $Na_{0.2}Ce(OH)_{2.4}(PO_4)_{0.6} \cdot nH_2O$ in the case of the sample obtained as a result of 15 SILD cycles. In our opinion, the formation of such microtubes occurs at the stage of sample drying due to the fact that the outer part of the synthesized coating with respect to the substrate has a lower density than that which is in contact with the substrate. Apparently, this occurs because the inner part of the layer was in contact with reagents for a longer time in total than the outer one. It is also impossible to exclude the reason for the increase in the coating density due to the formation of various cerium silicates in the contact zone with the substrate due to partial dissolution of an ultra-thin oxide nanolayer on the silicon

surface in an alkaline solution of Na_3PO_4. The obtained results, in our opinion, are one of the examples of the formation of microtubes of inorganic compounds during the drying of planar films with a density gradient across the thickness. Previously, we observed similar effects using microtubes with other wall compositions [23, 24]. It can be assumed that this effect of the formation of microtubes of inorganic compounds with a microscroll morphology is similar to the effect of the formation of nanotubes with a nanoscroll morphology, which the authors observed in [25,26] during their synthesis under hydrothermal conditions. However, in these cases, the twisting of the nanoscrolls was primarily the result of forces that arose due to differences in the structural properties of individual metal-oxygen polyhedra within their walls.

It is noteworthy that the coatings obtained as a result of 15 SILD cycles are most likely to twist. Apparently, the thin films of greater thickness are already more mechanically strong and the forces that arise during drying are no longer sufficient for the layer to twist. On the other hand, the thin films with a smaller thickness are less mechanically strong and when they are dried, such forces are not yet strong enough for their twisting. In addition, we have noticed that even if such thin films partially "twist", the microtubes that form them are not mechanically strong enough and they "collapse" into planar structures.

Additional and practically significant information can be obtained by analyzing the DR spectra of coatings on the surface of fused quartz (Fig. 4(b)). In these spectra, a wide absorption band can be observed in the range of 200–400 nm with an intensity increasing in a series of samples obtained as a result of a greater number of SILD cycles. This absorption band corresponds to charge-transfer transitions between the O($2p$) and Ce($4f$) states [27]. It is characteristic that already after 15 SILD cycles, a significant absorption of UV radiation at a level of 90 percent in the middle UV region, i.e., region B, is achieved. And this fact, in our opinion, opens up new possibilities for the creation of new, more effective absorbers of such radiation. Moreover, the optical properties of such coatings can be improved by doping their composition with various cations and anions. This doping can be relatively easily accomplished by using reagent solutions containing additives of various salts during synthesis. In particular, we have carried out test syntheses using solutions of salt mixtures and have shown that Fe(II) cations can be introduced into the composition up to an atomic concentration of 40%, as well as tungstate anions up to a value of 10% relative to the content of cerium atoms. A more detailed presentation of these experiments, however, goes far beyond the scope of this article and is therefore not presented here.

4. Conclusion

Successive and alternating treatment of silicon and quartz surfaces using the SILD technique with $(NH_4)_4Ce(SO_4)_4$ and NaH_2PO_4 solutions results in the formation of a $Ce(OH)PO_4 \cdot nH_2O$ coating with an amorphous crystalline structure. If a Na_3PO_4 solution is used as a reagent instead of NaH_2PO_4, the formation of $Na_{0.2}Ce(OH)_{2.4}(PO_4)_{0.6} \cdot nH_2O$ coatings with an amorphous structure is observed on the substrate surface. It is characteristic that in a series of $Na_{0.2}Ce(OH)_{2.4}(PO_4)_{0.6} \cdot nH_2O$ samples differing in the number of SILD cycles, the planar morphology of coatings can be disrupted for the sample obtained as a result of 15 SILD cycles. As it turnes out, formation of microtubes (microscrolls) is observed on the surface of such a sample due to the "twisting" of individual fragments of the synthesized thin film. The composition of the noted Ce(IV) phosphates can be doped with various cations and anions by adding corresponding salts to reagent solutions. This was demonstrated using Fe(II) cations and WO_4^{2-} anions as an example. The study of $Ce(OH)PO_4$ coatings by DR spectroscopy indicates the possibility of creating effective UV absorbers in the mid-B spectral range based on these coatings.

References

[1] Labrador-Paez L., Kostiv U., Widengren J. Liu H. Water: An Influential Agent for Lanthanide-Doped Luminescent Nanoparticles in Nanomedicine. *Adv. Optical Mater.*, 2023, **11**, P. 2200513.

[2] Enikeeva M.O., Proskurina O.V., Gerasimov E.Yu. Nevedomskiy V.N., Gusarov V.V. Synthesis in hydrothermal conditions and structural transformations of nanocrystals in the $LaPO_4$-YPO_4-(H_2O) system. *Nanosyst.: Phys., Chem., Math.*, 2023, **14**(6), P. 660–667.

[3] Martinon T.L.M., Pierre V.C. Luminescent Lanthanide Probes for Inorganic and Organic Phosphates. *Chem. Asian J.*, 2022, **17**, P. e202200495.

[4] Enikeeva M.O., Yakovleva A.A., Proskurina O.V. Nevedomskiy V.N., Gusarov V.V. Phase formation under hydrothermal conditions and thermal transformations in the $GdPO_4$-YPO_4-H_2O system. *Inorg. Chem. Commun.*, 2024, **159**, P. 111777.

[5] Enikeeva M.O., Zhidomorova K.A., Danilovich D.P., Nevedomskiy V.N., Proskurina O.V., Gusarov V.V. Phase formation and thermal analysis in the $LaPO_4$-$GdPO_4$-H_2O system. *Nanosyst.: Phys., Chem., Math.*, 2024, **15**(6), P. 781–792.

[6] Ruwaid Rafiuddin M., Donato G., McCaugherty S., Mesbah A., Grosvenor A.P. Review of Rare-Earth Phosphate Materials for Nuclear Waste Sequestration Applications. *ACS Omega*, 2022, **7**(44), P. 39482–39490.

[7] Kozlova T.O., Baranchikov A.E., Ivanov V.K. Cerium (IV) Orthophosphates. *Russ. J. of Inorg. Chem.*, 2021, **66**(12), P. 1761–1778.

[8] Marszałek M., Piotrowski M., Dziełak B., Blicharz M., Malarska W., Wzorek Z. Titanium(IV), Zirconium(IV), and Cerium(IV) Phosphates Synthesized Under Mild Conditions-Composition Characteristics and Evaluation of Sorption Properties Towards Copper Ions in Comparison to Commercially Available Ion-Exchange Resins. *Mater.*, 2024, **17**(24), P. 6226.

[9] Romanchuk A.Y., Shekunova T.O., Larina A.I., Ivanova O.S., Baranchikov A.E., Ivanov V.K., Kalmykov S.N. Sorption of Radionuclides onto Cerium (IV) Hydrogen Phosphate $Ce(PO_4)(HPO_4)_{0.5}(H_2O)_{0.5}$, Radiochem., 2019, **61**(6), P. 719–723.

[10] Popov A.L., Shcherbakov A.B., Zholobak N.M., Baranchikov A.Y., Ivanov V.K. Cerium dioxide nanoparticles as third-generation enzymes (nanozymes). *Nanosyst.: Phys. Chem. Math.*, 2017, **8**(6), P. 760–781.

[11] Ta K.M., Neal C.J., Coathup M.J., Seal S., Phillips R.M., Molinari M. The interaction of phosphate species with cerium oxide: The known, the ambiguous and the unexplained. *Biomater. Adv.*, 2025, **166**, P. 214063.

[12] Komiyama M. Ce-based solid-phase catalysts for phosphate hydrolysis as new tools for next-generation nanoarchitectonics. *Sci. Technol. Adv. Mater.*, 2023, **24**(1), P. 2250705.
[13] Kolesnik I.V., Shcherbakov A.B., Kozlova T.O., Kozlov D.A., Ivanov V.K. Comparative Analysis of Sun Protection Characteristics of Nanocrystalline Cerium Dioxide. *Russ. J. of Inorg. Chem.*, 2020, **65**(7), P. 960–966.
[14] Parwaiz S., Khan M.M., and Pradhan D. CeO_2-based nanocomposites: An advanced alternative to TiO2 and ZnO in sunscreens. *Mater. Express*, 2019, **9**(3), P. 185–202.
[15] Averochkin E.P., Steparuk A.S., Tekshina E.V. et al. Photoactive Layers based on ZnO Nanorods Obtained by Hydrothermal Synthesis for Dye-Sensitized Solar Cells. *Russ. J. Inorg. Chem.*, 2024, **69**, P. 925–932.
[16] Bulyarskiy S.V., Koiva D.A., Gusarov G.G., Svetukhin V.V. Changes in the titanium oxide optical properties during crystallization. *Opt. and Spectr.*, 2022, **130**(14), P. 2148.
[17] Kozlova T.O., Popov A.L., Kolesnik I.V., Kolmanovich D.D., Baranchikov A.E., Shcherbakov A.B., Ivanov V.K. Amorphous and crystalline cerium(IV) phosphates. *J. Mater. Chem. B*, 2022, **10**(11), P. 1775–1785.
[18] Gulina L.B., Pchelkina A.A., Nikolaev K.G., Navolotskaya D.V., Ermakov S.S., Tolstoy V.P. A brief review on immobilization of gold nanoparticles on inorganic surfaces and Successive Ionic Layer Deposition. *Rev. Adv. Mater. Sci.*, 2016, **44**(1), P. 46–53.
[19] Baranchikov A.E., Kozlova T.O., Istomin S.Y., Mironov A.V., Vasilchikova T.M., Gippius A.A., Plakhova T.V., Vasilyeva D.N., Ivanov, V.K. Sodium Cerium Phosphate, $(Na,Ce)_2Ce(PO_4)_2 \cdot xH_2O$, with Mixed Cerium Oxidation States. *ChemistrySelect*, 2024, **9**(17), P. e202401010.
[20] Kozlova T.O., Mironov A.V., Istomin S.Y., Birichevskaya K.V., Gippius A.A., Zhurenko S.V., Shatalova T.B., Baranchikov A.E., Ivanov V.K. Meet the Cerium (IV) Phosphate Sisters: $CeIV(OH)PO_4$ and $CeIV_2O(PO_4)_2$. *Chem. Eur. J.*, 2020, **26**(53), P. 12188–12193.
[21] Kozlova T.O., Vasilyeva D.N., Kozlov D.A., Teplonogova M.A., Baranchikov A.E., Simonenko N.P., Ivanov V.K. Synthesis and thermal behavior of $KCe_2(PO_4)_3$, a new full-member in the $AIMIV_2(PO_4)_3$ family. *Nanosyst.: Phys. Chem. Math.*, 2023, **14**(1), P. 112–119.
[22] Yin S., Saito M., Liu X., Sato T. Preparation and Characterization of Plate-like Cerium Phosphate/Nanosize Calcia Doped Ceria Composites by Precipitation Method. *Phosphorus Res. Bull.*, 2011, **25**, P. 68–71.
[23] Gulina L.B., Tolstoy V.P., Solovev A.A., Gurenko V.E., Huang G., Mei Y. Gas-Solution Interface Technique as a simple method to produce inorganic microtubes with scroll morphology. *Prog. Nat. Sci: Mater. Int.*, 2020, **30**(3), P. 279–288.
[24] Tolstoy V., Nikitin K., Kuzin A., Zhu F., Li X., Goltsman G., Gorin D., Huang G., Mei Y. Rapid synthesis of Pt (0) motors-microscrolls on a nickel surface via H_2PtCl_6-induced galvanic replacement reaction. *Chem. Commun.*, 2024, **60**(23), P. 3182–3185.
[25] Li Y., Liu X., Ji T., Zhang M., Yan X., Yao M., Sheng D., Li S., Ren P., Shen Z. Potassium ion doped manganese oxide nanoscrolls enhanced the performance of aqueous zinc-ion batteries. *Chinese Chem. Lett.*, 2025, **36**(1), P. 109551.
[26] Hettler S., Roy K.S., Arenal R., and Panchakarla L.S. Stable CoO_2 Nanoscrolls with Outstanding Electrical Properties. *Adv. Mater. Interfaces*, 2024, P. 2400317.
[27] Wang W., Zhang B., Jiang S., Bai H., Zhang S. Use of CeO_2 Nanoparticles to Enhance UV-Shielding of Transparent Regenerated Cellulose Films. *Polymers*, 2019, **11**(3), P. 458.

Submitted 4 October 2025; revised 25 November 2025; accepted 30 November 2025

Information about the authors:

Yuliana Chuvilo – Institute of Chemistry, Saint Petersburg State University, University St. 26, St. Peterhof, Saint Petersburg, 198504, Russia; st087011@student.spbu.ru

Leonid Kuklo – Institute of Chemistry, Saint Petersburg State University, University St. 26, St. Peterhof, Saint Petersburg, 198504, Russia; ORCID 0000-0002-7502-6788; lenkuklo@mail.ru

Valeri Tolstoy – Institute of Chemistry, Saint Petersburg State University, University St. 26, St. Peterhof, Saint Petersburg, 198504, Russia; ORCID 0000-0003-3857-7238; v.tolstoy@spbu.ru

Conflict of interest: the authors declare no conflict of interest.